Differential effects of partial and complete loss of TREM2 on microglial injury response and tauopathy

Faten A. Sayed[a,b,c], Maria Telpoukhovskaia[c], Lay Kodama[a,b,c], Yaqiao Li[c], Yungui Zhou[c], David Le[c], Axel Hauduc[c], Connor Ludwig[c], Fuying Gao[d,e], Claire Clelland[b,c], Lihong Zhan[c], Yonatan A. Cooper[f], Dimitrios Davalos[c,1], Katerina Akassoglou[b,c], Giovanni Coppola[d,e], and Li Gan[a,b,c,2]

[a]Neuroscience Graduate Program, University of California, San Francisco, CA 94158; [b]Department of Neurology, University of California, San Francisco, CA 94158; [c]Gladstone Institute of Neurological Disease, San Francisco, CA 94158; [d]Department of Psychiatry, Semel Institute for Neuroscience and Human Behavior, David Geffen School of Medicine, University of California, Los Angeles, CA 90095; [e]Departmentof Neurology, University of California, Los Angeles, CA 90095; and [f]Human Genetics and Genomics Graduate Program, University of California, Los Angeles, CA 90095

Edited by Don W. Cleveland, University of California, San Diego, La Jolla, CA, and approved August 23, 2018 (received for review July 6, 2018)

Alzheimer's disease (AD), the most common form of dementia, is characterized by the abnormal accumulation of amyloid plaques and hyperphosphorylated tau aggregates, as well as microgliosis. Hemizygous missense variants in Triggering Receptor Expressed on Myeloid Cells 2 (*TREM2*) are associated with elevated risk for developing late-onset AD. These variants are hypothesized to result in loss of function, mimicking TREM2 haploinsufficiency. However, the consequences of TREM2 haploinsufficiency on tau pathology and microglial function remain unknown. We report the effects of partial and complete loss of TREM2 on microglial function and tau-associated deficits. In vivo imaging revealed that microglia from aged TREM2-haploinsufficient mice show a greater impairment in their injury response compared with microglia from aged TREM2-KO mice. In transgenic mice expressing mutant human tau, TREM2 haploinsufficiency, but not complete loss of TREM2, increased tau pathology. In addition, whereas complete TREM2 deficiency protected against tau-mediated microglial activation and atrophy, TREM2 haploinsufficiency elevated expression of proinflammatory markers and exacerbated atrophy at a late stage of disease. The differential effects of partial and complete loss of TREM2 on microglial function and tau pathology provide important insights into the critical role of TREM2 in AD pathogenesis.

inflammation | motility | neurodegeneration | tau inclusions | RNA-seq

Alzheimer's disease (AD), the most common form of dementia, is characterized pathologically by the abnormal accumulation of amyloid plaques, hyperphosphorylated tau aggregates, and microgliosis. The recent genetic implication of a microglial-expressed gene, Triggering Receptor Expressed on Myeloid Cells 2 (*TREM2*), in late-onset AD suggests a pivotal role for microglia in AD pathogenesis. Although mutations in *TREM2* are rare, this gene is nonetheless the strongest immune gene-specific risk factor for AD discovered thus far (1–3). *TREM2* encodes a transmembrane receptor that is expressed by microglia in the brain (4, 5). TREM2 has been implicated in neuroinflammation and in the metabolic fitness, proliferation, survival, and phagocytic capacity of microglia (6–16).

The most common AD-associated *TREM2* variant, R47H, is associated with an approximately threefold increased risk for developing late-onset AD (1–3). It is thought to result in a TREM2 loss-of-function phenotype (10, 17, 18). Compared with noncarriers, R47H carriers have higher levels of phosphorylated tau around plaques (19) and more neurofibrillary tangles (20). In addition, R47H carriers have higher levels of cerebrospinal fluid (CSF)-soluble TREM2, and CSF-soluble TREM2 levels were significantly correlated with higher levels of CSF-phosphorylated tau (21). These observations in human patients suggest a detrimental effect of TREM2 haploinsufficiency on tau pathology. Surprisingly, in a tauopathy mouse model, complete loss of TREM2 function had no effect on tau pathology, while protecting against brain atrophy (22). These findings highlight the need to assess the effects of TREM2 haploinsufficiency in AD models.

We investigated how TREM2 haploinsufficiency, a model relevant to AD cases carrying hemizygous risk variants, affects microglial function and tau pathology. By using in vivo two-photon microscopy to visualize microglial motility, we found that TREM2 haploinsufficiency resulted in an age-dependent impairment in microglial injury response without affecting baseline motility. Interestingly, complete loss of TREM2 resulted in a milder impairment in injury-induced motility compared with TREM2 haploinsufficiency. We then investigated the effects of TREM2 haploinsufficiency and complete deficiency on tau pathology in mice expressing mutant human tau (P301S). Our findings demonstrated a robust increase in tau pathology in TREM2-haploinsufficient mice, an effect that was not observed in TREM2-KO mice. We further investigated how TREM2 haploinsufficiency and complete deficiency affect tau-mediated deficits.

Significance

Late-onset Alzheimer's disease is the most common form of dementia. A rare hemizygous variant in a microglial-expressed gene, Triggering Receptor Expressed on Myeloid Cells 2 (*TREM2*), significantly increases risk for late-onset Alzheimer's disease. This variant is thought to cause loss of function, inducing TREM2 haploinsufficiency. The ramifications of TREM2 haploinsufficiency on microglial function and tau pathology are major gaps in the field. We find that, in contrast to the protective effects of complete TREM2 deficiency, TREM2 haploinsufficiency exacerbates tau pathology, inflammation, and atrophy at a late stage of disease in a mouse model of tauopathy. The differential effects of partial and complete loss of TREM2 are important considerations for TREM2-targeted therapeutic strategies.

Author contributions: F.A.S. and L.G. designed research; F.A.S., Y.Z., D.L., A.H., and D.D. performed research; M.T., C.L., L.Z., Y.A.C., K.A., and G.C. contributed new reagents/analytic tools; F.A.S., M.T., L.K., Y.L., A.H., F.G., and L.G. analyzed data; and F.A.S., C.C., and L.G. wrote the paper.

The authors declare no conflict of interest.

This article is a PNAS Direct Submission.

Data deposition: The data reported in this paper have been deposited in the Gene Expression Omnibus (GEO) database, https://www.ncbi.nlm.nih.gov/geo (accession no. GSE118630).

[1]Present address: Department of Neurosciences, Lerner Research Institute, Cleveland Clinic, Cleveland, OH 44195.

[2]To whom correspondence should be addressed. Email: lgan@gladstone.ucsf.edu.

This article contains supporting information online at www.pnas.org/lookup/suppl/doi:10.1073/pnas.1811411115/-/DCSupplemental.

Published online September 19, 2018.

Results

TREM2 Haploinsufficiency Causes an Age-Dependent Impairment in Microglia's Injury Response. Microglia carry out critical functions of surveying the brain and responding to injury (23, 24). To address the effect of TREM2 on microglial surveillance, we used in vivo two-photon imaging to examine microglial motility in 3–5-mo-old *TREM2*$^{+/+}$, *TREM2*$^{+/-}$ and *TREM2*$^{-/-}$ mice crossed to *Cx3cr1*$^{GFP/+}$ mice, in which microglia express enhanced GFP driven by the *Cx3cr1* promoter (25). Analysis of a 10-min time-lapse recording of cortical microglia showed no differences in the baseline properties of microglia across the three genotypes, including average speed of process extension and retraction and total change in process length (Fig. 1 *A* and *B*). TREM2 also had no effect on microglial cell density or cell body size at baseline (*SI Appendix*, Fig. S1 *A* and *B*). Moreover, in response to a laser-induced focal tissue injury, microglia from young *TREM2*$^{+/+}$, *TREM2*$^{+/-}$ and *TREM2*$^{-/-}$ mice exhibited no difference in cell density (Fig. 1*C*), cell body size (*SI Appendix*, Fig. S1*C*), or the density of microglial processes extending toward the injury site (Fig. 1 *D* and *E* and Movie S1).

Given the established association of TREM2 with age-related diseases (1–3, 26), we next examined the effects of TREM2 on microglial motility in 9–14-mo-old *TREM2*$^{+/+}$, *TREM2*$^{+/-}$ and *TREM2*$^{-/-}$ mice. At baseline, the average speed and total change in process length did not differ across genotypes (Fig. 1 *F* and *G*). Microglial cell density or cell body size also remained similar (*SI Appendix*, Fig. S1 *D* and *E*). Strikingly, in response to focal tissue injury, microglia from older *TREM2*$^{+/-}$ mice exhibited a significantly reduced response to injury compared with WT microglia, as evidenced by fewer microglial processes extending toward the site of injury at any given time point (Fig. 1 *I* and *J* and Movie S2). *TREM2*$^{-/-}$ microglia showed a significant, yet milder, attenuation in response size compared with *TREM2*$^{+/-}$ (Fig. 1 *I* and *J* and Movie S2). *TREM2*$^{+/-}$ microglia were the slowest to respond, extended the fewest processes toward the site of injury, and did not reach the injury site within 60 min (Fig. 1*I* and Movie S2). *TREM2*$^{-/-}$ microglia, on the contrary, were able to reach the injury site within 60 min, similar to WT microglia (Fig. 1*I* and Movie S2). The impairment in *TREM2*$^{+/-}$ and *TREM2*$^{-/-}$ microglia responses were not associated with differences in microglial density (Fig. 1*H*) or activation state, as evidenced by the unaltered cell body size (*SI Appendix*, Fig. S1*F*). Moreover, there was no correlation between ablation size and response (*SI Appendix*, Fig. S1*G*), indicating that the reduced response sizes in TREM2-deficient microglia were not caused by smaller injuries. Thus, surprisingly, TREM2 haploinsufficiency attenuates the in vivo microglial response to tissue injury in an age-dependent manner and to a greater extent than complete TREM2 deficiency.

TREM2 Haploinsufficiency and Complete Deficiency Differentially Regulate the Microglial Transcriptome in the Presence and Absence of Tauopathy. Next, to identify microglial pathways regulated by *TREM2* in an unbiased fashion, we performed RNA sequencing (RNA-seq) of adult microglia isolated by using CD11b magnetic beads from young *TREM2*$^{+/+}$, *TREM2*$^{+/-}$ and *TREM2*$^{-/-}$ mice. We confirmed the purity of our adult-isolated microglia, as their transcriptome closely matched a previously published microglial transcriptome (27) (Fig. 2*A*). TREM2 haploinsufficiency and complete deficiency altered the microglial transcriptome in unique ways (Fig. 2*B*). A total of 107 transcripts were significantly different between *TREM2*$^{+/-}$ and *TREM2*$^{-/-}$ (Fig. 2*C*). Ingenuity Pathway Analysis (IPA) revealed cellular movement as the most significantly altered biological pathway in *TREM2*$^{+/-}$ microglia compared with *TREM2*$^{-/-}$ (Fig. 2*D*), consistent with our in vivo imaging finding that *TREM2*$^{+/-}$ microglia exhibited greater impairment in their injury response than *TREM2*$^{-/-}$ (Fig. 1*J*). Interestingly, these transcriptomic alterations in young *TREM2*$^{+/-}$ microglia preceded the impaired injury response seen in aged *TREM2*$^{+/-}$ microglia. In addition, multiple pathways pertaining to inflammation were significantly altered between *TREM2*$^{+/-}$ and *TREM2*$^{-/-}$ microglia, such as immune cell trafficking and inflammatory response (Fig. 2*D*), suggesting differential regulation of inflammation in TREM2$^{+/-}$ vs. *TREM2*$^{-/-}$ microglia.

The rare R47H missense variant in *TREM2* is associated with increased risk for tauopathies (2, 3, 26, 28) and hyperphosphorylation

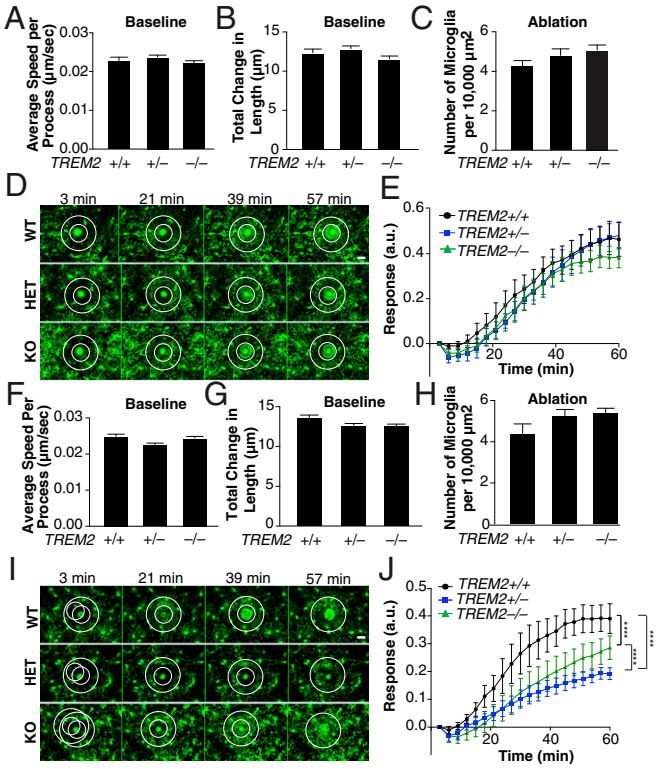

Fig. 1. TREM2 haploinsufficiency causes an age-dependent impairment of microglia's injury response in vivo. (*A–E*) Quantification of microglial motility in 3–5-mo-old mice. Quantification of the average speed per microglial process (*A*) and total change in length of microglial processes (*B*) during 10-min baseline recordings from 3–5-mo-old mice. *TREM2*$^{+/+}$, $n = 7$ recordings from 7 mice; *TREM2*$^{+/-}$, $n = 9$ recordings from 9 mice; *TREM2*$^{-/-}$, $n = 10$ recordings from 10 mice. (*C*) Microglial density for young mice from laser-induced tissue injury videos. *TREM2*$^{+/+}$, $n = 10$ recordings from 9 mice; *TREM2*$^{+/-}$, $n = 11$ recordings from 10 mice; *TREM2*$^{-/-}$, $n = 12$ recordings from 10 mice. (*D*) Representative still images at 3 min, 21 min, 39 min, and 57 min from the microglial responses to injury in young mice. Laser ablations are outlined with smaller white circles. The response was normalized to microglial density at each time point, denoted by larger white circles. (Scale bar: 20 μm.) (*E*) Quantification of normalized microglial responses from young mice toward focal laser-induced tissue injury over a period of 60 min from time of injury. *TREM2*$^{+/+}$, $n = 7$ injuries from 7 mice; *TREM2*$^{+/-}$, $n = 11$ injuries from 10 mice; *TREM2*$^{-/-}$, $n = 12$ injuries from 10 mice. (*F–H*) Quantification of microglial motility in 9–14-mo old mice. (*F*) Quantification of the average speed per microglial process and (*G*) total change in length of processes during 10-min baseline recordings from 9–14-mo-old mice. *TREM2*$^{+/+}$, $n = 10$ recordings from 7 mice; *TREM2*$^{+/-}$, $n = 10$ recordings from 9 mice; *TREM2*$^{-/-}$, $n = 10$ recordings from 9 mice. (*H*) Microglial density for aged mice during laser-induced tissue injury experiments. *TREM2*$^{+/+}$, $n = 7$ recordings from 6 mice; *TREM2*$^{+/-}$, $n = 13$ recordings from 10 mice; *TREM2*$^{-/-}$, $n = 12$ recordings from 9 mice. (*I*) Representative still images at 3 min, 21 min, 39 min, and 57 min from the microglial responses to injury in aged mice. Laser ablations are outlined with smaller white circles. Response size was normalized to microglial density at each time point, denoted by larger white circles. (Scale bar: 20 μm.) (*J*) Quantification of normalized microglial responses from aged mice toward focal laser-induced tissue injury was measured over a period of 60 min from time of injury. *TREM2*$^{+/+}$, $n = 6$ injuries from 5 mice; *TREM2*$^{+/-}$, $n = 13$ injuries from 10 mice; *TREM2*$^{-/-}$, $n = 12$ injuries from 9 mice (****$P < 0.0001$, STATA mixed-effects modeling). Values are expressed as mean ± SEM. Data were analyzed using one-way ANOVA with Bonferroni post hoc analyses for all panels except for *E* and *J*, which were analyzed by using STATA mixed-effects modeling.

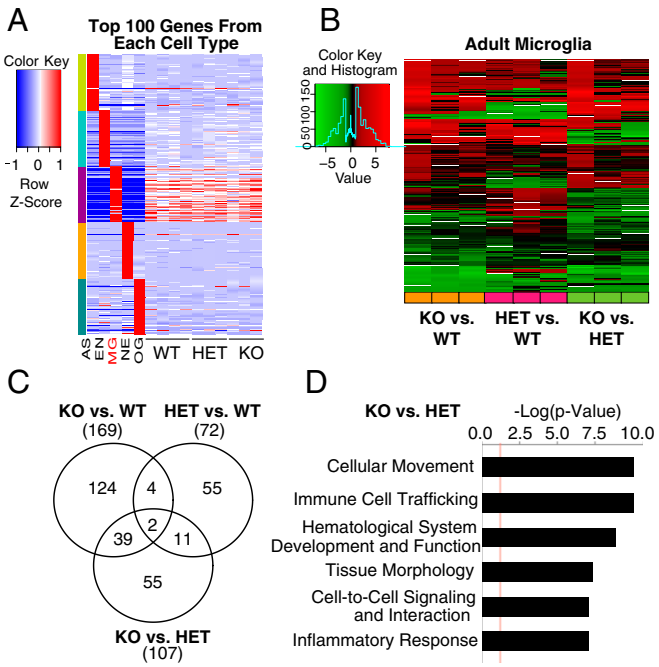

Fig. 2. Differential effects of partial and complete loss of TREM2 on the microglial transcriptome. (*A*) RNA-seq of microglia isolated from the forebrain of 3–4-mo-old mice ($TREM2^{+/+}$, $n = 4$ samples from 8 mice; $TREM2^{+/-}$, $n = 3$ samples from 6 mice; $TREM2^{-/-}$, $n = 3$ samples from 6 mice). Expression levels of the top 100 most enriched transcripts in astrocytes (AS), endothelial cells (EN), microglia (MG), neurons (NE), and oligodendrocytes (OG), as identified by Zhang et al. (27). Columns 1–5: data from Zhang et al. Columns 6–15: expression data in microglia from $TREM2^{+/+}$, $TREM2^{+/-}$, and $TREM2^{-/-}$ mice. Shades of red correspond to increased levels compared with average gene expression, and shades of blue correspond to decreased levels. (*B*) Heat map representing significantly altered transcripts ($P < 0.005$) across all genotypes. Samples are in columns and genes are in rows. Shades of red represent up-regulation, and shades of green represent down-regulation. (*C*) Venn diagram illustrating the number and overlap of transcripts that were significantly altered between the two indicated genotypes ($P < 0.005$). (*D*) IPA of top six enriched disease and biological function pathways from 107 transcripts that were significantly altered in $TREM2^{-/-}$ microglia compared with $TREM2^{+/-}$ microglia ($P < 0.005$). Bars indicate −log (*P* value) of enrichment. Red dotted line corresponds to $P = 0.05$.

of tau in AD carriers (19). We next investigated how TREM2 affects tau pathology and tau-associated deficits in the P301S tauopathy mouse model (Prnp-MAPT*P301S) (29). The effects of TREM2 haploinsufficiency and complete loss of TREM2 on tau-induced transcriptional changes were examined at 8–9 mo of age (*SI Appendix*, Fig. S2*A*), when P301S mice exhibit significant tau inclusions, microgliosis, and neuronal loss (29). Compared with $P301S^{+}$ $TREM2^{+/+}$ mice, there were 232 differentially expressed transcripts in $P301S^{+}$ $TREM2^{+/-}$ mice (Fig. 3*A*). These transcripts were significantly enriched for pathways pertaining to microglial development, such as TGFβ signaling (4), and inflammation, such as IL2 STAT5 signaling and TNF-α signaling via NF-κB (*SI Appendix*, Fig. S2*B*). To validate these pathways, we performed quantitative real-time PCR of pro- and anti-inflammatory markers. Consistent with tau-mediated inflammatory responses, expression of P301S human tau significantly increased levels of proinflammatory cytokines TNF-α, IL-1α, and IL-1β (*SI Appendix*, Fig. S3). Importantly, $TREM2^{+/-}$ resulted in significantly elevated levels of TNF-α and IL-1α compared with $P301S^{+}$ $TREM2^{+/+}$ mice, but had no effects on anti-inflammatory markers VEGF1, Cox2, or IL-34 (*SI Appendix*, Fig. S3). Differentially expressed genes in $P301S^{+}$ $TREM2^{-/-}$ on the contrary, were significantly enriched for genes related to metabolism, such as oxidative phosphorylation, glycolysis, and MTORC1 signaling (*SI Appendix*, Fig. S2*C*). Direct comparison of $P301S^{+}$ $TREM2^{+/-}$ and $P301S^{+}$ $TREM2^{-/-}$ revealed that, of the 389 differentially expressed transcripts, there was a significant enrichment of complement-related genes and inflammatory response genes (Fig. 3*B*).

TREM2 Haploinsufficiency Exacerbates Tau Pathology in P301S Mice. We then assessed how partial and complete loss of TREM2 affects tau aggregation. Immunohistochemistry with the AT8 antibody, which recognizes two phosphorylation sites on tau (pS202, pT205), revealed a significant increase in the $AT8^{+}$ area in the cortex of $P301S^{+}$ $TREM2^{+/-}$ mice compared with $P301S^{+}$ $TREM2^{+/+}$ and $P301S^{+}$ $TREM2^{-/-}$ (Fig. 4 *A* and *B*) and a trend toward increased AT8 pathology in the hippocampus (Fig. 4 *C* and *D*). In contrast, there was no difference in AT8 load between $P301S^{+}$ $TREM2^{-/-}$ and $P301S^{+}$ $TREM2^{+/+}$ mice in hippocampus and cortex (Fig. 4 *A*–*D*), consistent with a recent finding by Leyns et al. (22). We also performed immunohistochemistry with the MC1 antibody, which detects a pathological conformation of tau (30). Consistent with the differential effects induced by $TREM2^{+/-}$ and $TREM2^{-/-}$ on AT8 pathology, $P301S^{+}$ $TREM2^{+/-}$ mice had significantly greater $MC1^{+}$ area than $P301S^{+}$ $TREM2^{-/-}$ in cortex (Fig. 4 *E* and *F*) and in hippocampus (Fig. 4 *G* and *H*). Similarly, the $MC1^{+}$ area in the hippocampus of $P301S^{+}$ $TREM2^{+/-}$ mice, most notably in the mossy fibers, was significantly greater than in $P301S^{+}$ $TREM2^{+/+}$ mice (Fig. 4 *G* and *H*). A similar trend was observed in the cortex (Fig. 4 *E* and *F*). In sharp contrast, the $MC1^{+}$ area trended toward a decrease in $P301S^{+}$ $TREM2^{-/-}$ mice compared with $P301S^{+}$ $TREM2^{+/+}$ mice (Fig. 4 *F* and *H*). Thus, TREM2 haploinsufficiency, but not complete loss of TREM2, enhances tau pathology.

Differential Effects of Partial and Complete TREM2 Deficiency on Atrophy and Microgliosis in P301S Mice. Next, we investigated how TREM2 haploinsufficiency and complete deficiency affect tau-induced neurodegeneration. At 8–9 mo of age, there were similar levels of hippocampal neuronal loss in P301S mice regardless of TREM2 genotype (*SI Appendix*, Fig. S4 *A* and *B*) and tau-induced atrophy could not yet be detected in cortex (*SI Appendix*, Fig. S4*C*). However, complete TREM2 deficiency resulted in a protection against hippocampal atrophy, as evidenced by the smaller lateral ventricle area (Fig. 5 *A* and *B*), and a trend toward increased hippocampal area (Fig. 5*C*). This result is in agreement with a previous report that showed that complete TREM2 deficiency protected against brain atrophy in P301S mice (22). Compared with $P301S^{+}$ $TREM2^{+/+}$, TREM2 haploinsufficiency did not significantly affect atrophy at 8–9 mo (Fig. 5

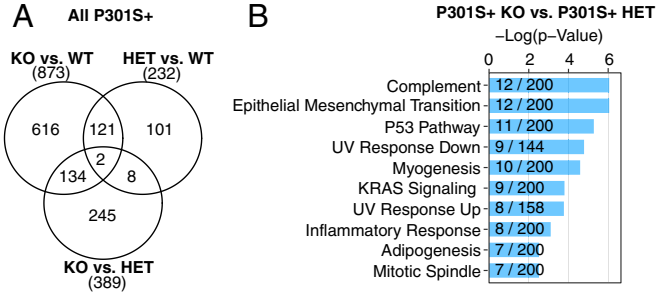

Fig. 3. Differential effects of partial and complete loss of TREM2 on P301S-induced transcriptional changes. (*A*) Venn diagram illustrating the number and overlap of transcripts that were significantly altered between the two indicated $P301S^{+}$ genotypes from 8–9-mo-old mice ($P < 0.005$, four mice per genotype, one mouse per sample). (*B*) Gene Set Enrichment Analysis (GSEA) using the hallmark database on significantly differentially expressed transcripts between partial vs. complete loss of TREM2 in P301S mice. The top 10 most enriched pathways are shown. The fraction on the bar graph indicates the total number of genes curated in the database for the specified term (denominator) and the number of overlapping genes in the inputted RNA-seq dataset (numerator).

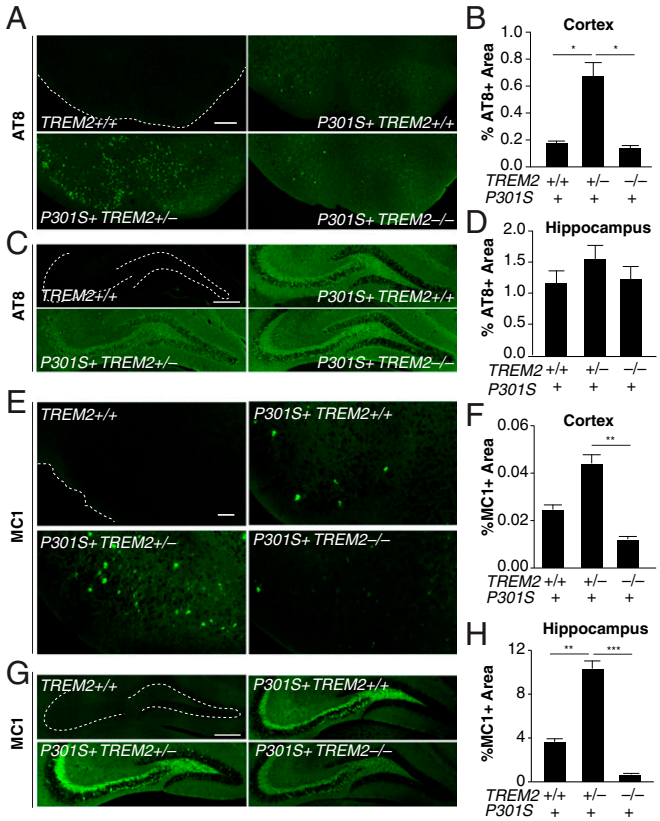

Fig. 4. TREM2 haploinsufficiency exacerbates tau pathology in P301S$^+$ mice. (*A*) Representative images of AT8 immunostaining in the cortex of 8–9-mo-old mice. (Scale bar: 100 μm.) (*B*) Quantification of the percentage of AT8$^+$ area in the cortex of P301S$^+$ *TREM2*$^{+/+}$, $n = 9$ mice; P301S$^+$ *TREM2*$^{+/-}$, $n = 25$ mice; P301S$^+$ *TREM2*$^{-/-}$, $n = 9$ mice; 6–8 sections per mouse (*$P <$ 0.05, STATA mixed-effects modeling). (*C*) Representative images of AT8 immunostaining in the hippocampus of 8–9-mo-old mice. (Scale bar: 300 μm.) (*D*) Quantification of the percentage of AT8$^+$ area in the hippocampus of P301S$^+$ *TREM2*$^{+/+}$, $n = 9$ mice; P301S$^+$ *TREM2*$^{+/-}$, $n = 25$ mice; P301S$^+$ *TREM2*$^{-/-}$, $n = 10$ mice; 6–8 sections per mouse. (*E*) Representative images of MC1 immunostaining in the cortex of 8–9-mo-old mice. (Scale bar: 300 μm.) (*F*) Quantification of the percentage of MC1$^+$ area in the cortex of P301S$^+$ *TREM2*$^{+/+}$, $n = 9$ mice; P301S$^+$ *TREM2*$^{+/-}$, $n = 25$ mice; P301S$^+$ *TREM2*$^{-/-}$, $n = 9$ mice; 7–16 sections per mouse (**$P < 0.01$, R mixed-effects modeling). (*G*) Representative images of MC1 immunostaining in the hippocampus of 8–9-mo-old mice. (Scale bar: 100 μm.) (*H*) Quantification of the percentage of MC1$^+$ area in the hippocampus of P301S$^+$ *TREM2*$^{+/+}$, $n = 9$ mice; P301S$^+$ *TREM2*$^{+/-}$, $n = 25$ mice; P301S$^+$ *TREM2*$^{-/-}$, $n =$ 10 mice; 7–16 sections/mouse (**$P < 0.01$, ***$P < 0.001$, R mixed-effects modeling). Values are expressed as mean ± SEM.

A–*C*) or at 10–11 mo of age (Fig. 5 *D* and *E*). However, compared with WT mice, *P301S*$^+$ *TREM2*$^{+/-}$, but not *P301S*$^+$ *TREM2*$^{+/+}$, mice exhibited significantly more severe atrophy (Fig. 5 *D* and *E*).

We next evaluated how TREM2 levels affect tau-induced microgliosis, a canonical hallmark of AD pathology recapitulated in P301S mice (29). Analysis of Iba1 immunoreactivity in the hippocampus revealed an expected significant increase in microglial number induced by P301S tau (Fig. 6 *A* and *B*). Interestingly, compared with P301S$^+$ *TREM2*$^{+/+}$, complete TREM2 deficiency, but not haploinsuffciency, resulted in a trend toward reduced microglial density (Fig. 6 *A* and *B*). Moreover, the number of microglia positively correlated with MC1$^+$ area (Fig. 6*C*), supporting the idea that elevated tau pathology is associated with inflammatory responses in microglia.

To further characterize how TREM2 levels affect tau-mediated microglial activation, we performed morphological analyses by using 3D renderings of confocal images (Fig. 6*D*). Compared with *TREM2*$^{+/+}$, TREM2 haploinsufficiency in P301S mice induced significantly shortened processes (Fig. 6*E*) and fewer branches (Fig. 6*F*), indicating strong tau-mediated microglial activation. In contrast, complete loss of TREM2 in P301S mice resulted in a failure to induce morphological changes associated with microglial activation; microglia from *P301S*$^+$ *TREM2*$^{-/-}$ mice exhibited similar process length and arborization as nonactivated microglia from WT (*TREM*$^{+/+}$) mice (Fig. 6 *D*–*F*).

Discussion

Our study highlights multiple findings in which TREM2 haploinsufficiency resulted in stronger or different phenotypes than complete TREM2 deficiency. TREM2 haploinsufficiency led to a greater age-dependent impairment in microglia response to injury compared with complete TREM2 deficiency. Moreover, TREM2 haploinsufficiency exacerbated tau pathology, atrophy, and inflammation. On the contrary, complete loss of TREM2 protected against atrophy and reduced microgliosis. Interestingly, complete loss of TREM2 was also associated with trends toward reduced MC1$^+$ pathology. These results highlight multiple TREM2 phenotypes that are gene-dose–independent. As hemizygous TREM2 variants are associated with elevated risk for AD, TREM2 haploinsufficiency may be a more relevant model to study how TREM2 contributes to AD pathogenesis. Indeed, complete loss of TREM2 in humans results in Nasu–Hakola disease (31), which could be driven by mechanisms that are distinct from those of AD.

As the resident immune cells in the brain, microglia need to respond robustly to injury, especially in neurodegenerative brains

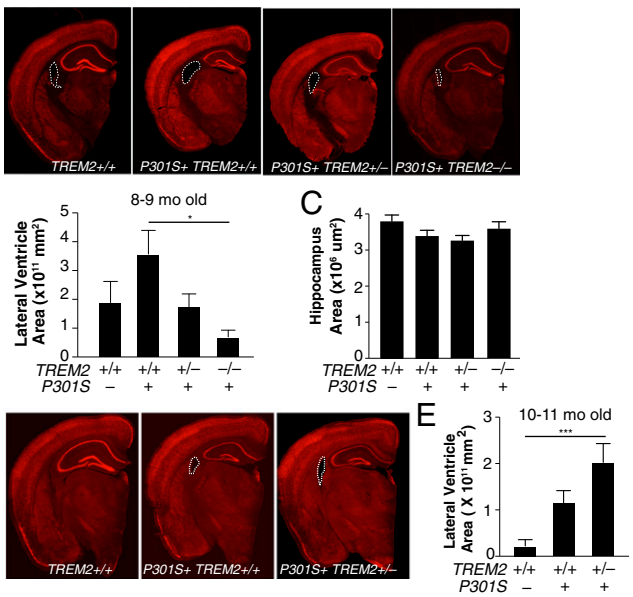

Fig. 5. Differential effects of partial and complete loss of TREM2 on atrophy in P301S$^+$ mice. (*A*) Representative images of NeuN immunostaining from 8–9-mo-old mice. Lateral ventricle outlined with a white dashed line. (*B*) Quantification of the lateral ventricle area of *TREM2*$^{+/+}$, $n = 6$ mice; P301S$^+$ *TREM2*$^{+/+}$, $n = 9$ mice; P301S$^+$ *TREM2*$^{+/-}$, $n = 25$ mice; P301S$^+$ *TREM2*$^{-/-}$, $n = 10$ mice, 6–17 sections per mouse (*$P < 0.05$, one-way ANOVA with Bonferroni post hoc analysis). (*C*) Quantification of the hippocampal area in 8–9-mo-old *TREM2*$^{+/+}$, $n = 6$; P301S$^+$ *TREM2*$^{+/+}$, $n = 9$; P301S$^+$ *TREM2*$^{+/-}$, $n = 25$; and P301S$^+$ *TREM2*$^{-/-}$, $n = 10$ mice, 6–17 sections per mouse. (*D*) Representative images of NeuN immunostaining from 10–11-mo-old mice. Lateral ventricle outlined with a white dashed line. (*E*) Quantification of the lateral ventricle area of *TREM2*$^{+/+}$, $n = 12$ mice; P301S$^+$ *TREM2*$^{+/+}$, $n = 12$ mice; P301S$^+$ *TREM2*$^{+/-}$, $n = 11$ mice; $n = 6$–8 sections per mouse (***$P < 0.001$, one-way ANOVA with Bonferroni post hoc analysis). Values are expressed as mean ± SEM.

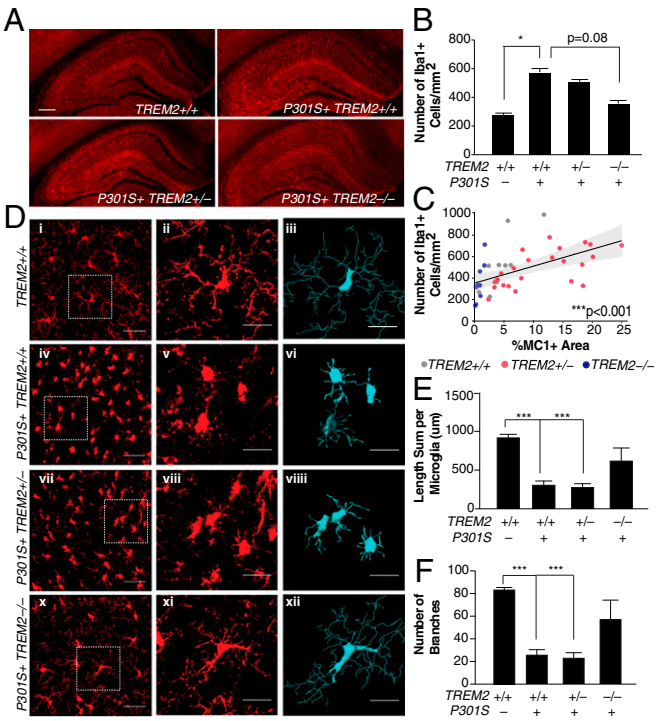

Fig. 6. Differential regulation of inflammation by partial and complete loss of TREM2 in P301S^{+} mice. (*A*) Representative images of Iba1 immunostaining of microglia in the hippocampus of 8–9-mo-old mice. (Scale bar: 300 μm.) (*B*) Quantification of the number of microglia per millimeter squared in the hippocampus of *TREM2*$^{+/+}$, $n = 5$ mice; P301S^{+} *TREM2*$^{+/+}$, $n = 9$ mice; P301S^{+} *TREM2*$^{+/-}$, $n = 25$ mice; P301S^{+} *TREM2*$^{-/-}$, $n = 10$ mice; 6–17 sections per mouse (*$P < 0.05$, R mixed-effects modeling). (*C*) Significant positive correlation between hippocampal percent MC1^{+} area and number of Iba1^{+} cells per square millimeter (***$P < 0.001$, linear regression). Each dot represents one animal. Graph depicts mean and 95% CIs. Genotypes are color-coded according to key. (*D*) Representative images of hippocampal Iba1 immunostaining and the corresponding 3D reconstructions using Imaris. (Scale bars: full-view images, 40 μm; magnified images, 20 μm.) (*E*) Quantification of the length sum of microglial processes and (*F*) number of microglial branches in *TREM2*$^{+/+}$, $n = 4$ mice (35 cells); P301S^{+} *TREM2*$^{+/+}$, $n = 7$ mice (123 cells); P301S^{+} *TREM2*$^{+/-}$, $n = 9$ mice (169 cells); P301S^{+} *TREM2*$^{-/-}$, $n = 5$ mice (64 cells; *$P < 0.05$ and ***$P < 0.001$, one-way ANOVA with Bonferroni post hoc analysis). Values are expressed as mean ± SEM.

that have increased neuronal death and accumulation of abnormal protein aggregates. By using in vivo imaging, we showed that TREM2 haploinsufficiency impairs microglia's injury-induced response in an age-dependent manner and to a greater degree than complete loss of TREM2 (Fig. 1*J* and Movie S2). It is interesting that this result is present in aged but not young mice. This finding mirrors the role of TREM2 in the development of late-onset AD. Notably, there was no impairment in baseline motility (Fig. 1 *F* and *G*), suggesting that TREM2 modulates microglial pathways specifically related to injury response. This injury-specific modulation of motility may contribute to TREM2's implication in neurodegeneration, in which neuronal injury is abundant. This type of differential modulation of baseline and injury-induced motility has been observed previously in the microglia field. For example, the purinergic receptor P2RY12 was found to slow down microglia's response to ATP/ADP released during injury without affecting baseline motility (32).

Aged TREM2-haploinsufficient microglia were significantly slower to respond to injury and extended fewer processes toward the site of injury throughout the 60-min imaging session (Movie S2). Interestingly, TREM2-deficient microglia showed an intermediate phenotype between TREM2 haploinsufficient and WT microglia. On average, they extended more processes toward the site of injury than TREM2-haploinsufficient microglia, and they were able to reach the site of injury within 60 min (Movie S2). This gene-dose–independent phenomenon may be driven by compensatory mechanisms in microglia completely lacking TREM2 from development, whereas TREM2 haploinsufficiency could elicit different types of compensatory changes via modulation of TREM2 expression from the existing allele. Our RNA-seq analyses of *TREM2*$^{+/-}$ and *TREM2*$^{-/-}$ microglia revealed a significant difference in the cellular movement pathway induced by TREM2 deficiency (Fig. 2*D*), consistent with a previous study that looked at *TREM2*$^{+/+}$ and *TREM2*$^{-/-}$ microglia (33). Interestingly, the transcriptional changes in TREM2-haploinsufficient microglia occurred before the development of the impaired injury response. These observations are consistent with a two-hit hypothesis: young TREM2-haploinsufficient microglia can maintain normal function, but those challenged by age or pathological conditions, such as tauopathy, are unable to do so.

Remarkably, TREM2 haploinsufficiency exacerbated tau pathology whereas complete TREM2 deficiency did not (Fig. 4), yet another phenotype that was not gene-dose–dependent. Of note, patients with the R47H TREM2 variant have increased tau pathology (13), similar to TREM2-haploinsufficient tauopathy mice. One likely explanation for the lack of effect of complete TREM2 deficiency on multiple phenotypes is that complete loss of TREM2 may result in compensatory changes. Indeed, a previous study showed that, in the absence of TREM2, expression of homeostatic microglial genes was not suppressed, but rather fully preserved and even slightly increased, supporting the possibility of compensation (33). Moreover, we observed transcriptional changes between *TREM2*$^{+/-}$ and *TREM2*$^{-/-}$ microglia that may underlie gene-dose–independent phenotypes. Inflammatory pathways were altered at the transcriptional level between *TREM2*$^{+/-}$ and *TREM2*$^{-/-}$ microglia from young mice (Fig. 2*D*), highlighting early-onset, inherent TREM2-dependent changes in microglial activation that persisted in older disease states (Fig. 6 and *SI Appendix*, Fig. S3).

The P301S mouse model begins to show neuronal loss at 9–10 mo of age (29). Neither TREM2 haploinsufficiency nor complete deficiency exacerbated neuronal loss at 8–9 mo of age. However, complete loss of TREM2 protected against tau-induced atrophy (Fig. 5 *A*–*C*). Our results suggest that the increase in cortical volume seen by Leyns et al. (22) may not be caused by a protection against neuronal loss per se, as P301S^{+} *TREM2*$^{-/-}$ mice had a similar number of neurons as P301S^{+} *TREM2*$^{+/+}$ mice (*SI Appendix*, Fig. S4*C*). Instead, complete loss of TREM2 may increase cortical volume through other mechanisms, such as protection against loss of neuronal processes or, given TREM2's implication in lipid sensing (10), through an increase in the brain's lipid content. In contrast to the neuroprotective effect of complete loss of TREM2, partial loss of TREM2 appears to be detrimental, highlighted by the significant increase in lateral ventricle area at 10–11 mo of age compared with WT mice (Fig. 5*E*). It is interesting to note that complete loss of TREM2 resulted in a trend toward reduced late-stage tau pathology and reduced atrophy, whereas TREM2 haploinsufficiency exacerbated tau pathology and exacerbated atrophy. It remains to be determined whether tau pathology and microglial activation work together or independently to cause brain atrophy.

We also detected increased expression of proinflammatory cytokines in P301S^{+} *TREM2*$^{+/-}$ mice (*SI Appendix*, Fig. S3), a finding consistent with the cytokine profiles in R47H carriers with AD (20). However, it is unclear whether the increased inflammatory state is a cause or consequence of the increased tau pathology present in *TREM2*$^{+/-}$ mice and patients with the R47H variant (19). Interestingly, in amyloid mouse models, TREM2 haploinsufficiency did not affect the expression of pro- or anti-inflammatory markers at early or later stages of amyloid pathology (8), but reduced microglia number (10). These studies, in conjunction with our data, suggest that TREM2 haploinsufficiency differentially modulates inflammation in the contexts of amyloid and tau pathology. On the contrary, P301S^{+} mice completely lacking

TREM2 have been shown to have lower levels of proinflammatory markers (22), as well as reduced microglial density and a resting state morphology. Together, these results, along with our RNA-seq data (Figs. 2*D* and 3*B* and *SI Appendix*, Fig. S2*B*), suggest inflammation as a possible mechanism by which TREM2 haploinsufficiency vs. complete deficiency result in apparent opposing phenotypes, such as their effects on tau pathology. Microglia have been implicated in the spread of tau pathology (34), and their activation state could contribute to how they respond in the context of tauopathy. Indeed, we found a significant positive correlation between microglial density and tau pathology (Fig. 6*C*).

Our surprising discovery that TREM2 haploinsufficiency exerts a more robust impairment in microglial function and exacerbation of tau pathology compared with complete loss of TREM2 highlights the plasticity of microglia in response to TREM2 deficiency. The potential detrimental effects of TREM2 haploinsufficiency can provide insight into how TREM2 contributes to AD pathogenesis and inform potential TREM2-targeted therapeutic strategies.

Methods

Detailed procedures for all methods described here are provided in the *SI Appendix*.

Mice. All animal procedures were carried out under protocols approved by the University of California, San Francisco, Institutional Animal Care and Use Committee.

In Vivo Imaging. Intravital imaging using two-photon microscopy was performed with thinned-skull windows as previously described (24).

Antibodies, Immunohistochemistry, and Image Analysis. Immunohistochemistry and image analysis were performed by experimenters blinded to the genotypes. The code was not broken until all analyses were completed.

Adult Microglia Isolation and Quantitative RT-PCR. Adult microglia were isolated from *TREM2*$^{+/+}$, *TREM2*$^{+/-}$ and *TREM2*$^{-/-}$ mice as described previously (35).

RNA-Seq and Analysis. RNA-seq libraries were prepared with Ovation RNA-seq system v2 kit (NuGEN) or Lexogen QuantSeq 3′ mRNA-Seq Library Prep Kit. All RNA-seq data have been deposited in the Gene Expression Omnibus repository (https://www.ncbi.nlm.nih.gov/geo/) under accession number GSE118630.

Statistical Analysis. Data were analyzed with GraphPad Prism v. 7 (GraphPad), STATA12 (StataCorp), or R (R Foundation for Statistical Computing). Multilevel mixed-effects linear regression model fit using STATA12 was used to compare curves for young and aged mice in response to injury. For cluster analyses of multiple measurements from individual mice, we used the R package lmer. Outliers were removed based on GraphPad's outlier analysis algorithm. All animals were included for statistical analyses unless otherwise noted.

ACKNOWLEDGMENTS. We thank Victoria Rafalski for her contribution in discussing the in vivo imaging work. All in vivo imaging was conducted by F.A.S. at the Center for In Vivo Imaging Research at Gladstone Institutes. Library preparation and quality control for adult microglia RNA-seq was conducted by Jim McGuire, PhD, at the Gladstone Genomics Core. RNA-seq was conducted by the University of California, San Francisco's Center for Advanced Technology. This study was supported by National Institute of Aging Grants AG051390 and R01AG054214 (to L.G.), National Institute of Neurological Diseases and Stroke Grant NS097976 (to K.A.), American Heart Association Scientist Development Grant 13SDG17210051 (to D.D.), National Institute of Neurological Diseases and Stroke Informatics Center for Neurogenetics and Neurogenomics Grant P30 NS062691 (to G.C.), and National Institute of Aging Grant F31 AG058505 (to F.A.S.).

1. Cruchaga C, et al.; GERAD Consortium; Alzheimer's Disease Neuroimaging Initiative (ADNI); Alzheimer Disease Genetic Consortium (ADGC) (2013) GWAS of cerebrospinal fluid tau levels identifies risk variants for Alzheimer's disease. *Neuron* 78:256–268.
2. Jonsson T, et al. (2013) Variant of TREM2 associated with the risk of Alzheimer's disease. *N Engl J Med* 368:107–116.
3. Guerreiro R, et al.; Alzheimer Genetic Analysis Group (2013) TREM2 variants in Alzheimer's disease. *N Engl J Med* 368:117–127.
4. Butovsky O, et al. (2014) Identification of a unique TGF-β-dependent molecular and functional signature in microglia. *Nat Neurosci* 17:131–143.
5. Hickman SE, et al. (2013) The microglial sensome revealed by direct RNA sequencing. *Nat Neurosci* 16:1896–1905.
6. Neumann H, Takahashi K (2007) Essential role of the microglial triggering receptor expressed on myeloid cells-2 (TREM2) for central nervous tissue immune homeostasis. *J Neuroimmunol* 184:92–99.
7. Hsieh CL, et al. (2009) A role for TREM2 ligands in the phagocytosis of apoptotic neuronal cells by microglia. *J Neurochem* 109:1144–1156.
8. Ulrich JD, et al. (2014) Altered microglial response to Aβ plaques in APPPS1-21 mice heterozygous for TREM2. *Mol Neurodegener* 9:20.
9. Poliani PL, et al. (2015) TREM2 sustains microglial expansion during aging and response to demyelination. *J Clin Invest* 125:2161–2170.
10. Wang Y, et al. (2015) TREM2 lipid sensing sustains the microglial response in an Alzheimer's disease model. *Cell* 160:1061–1071.
11. Zhong L, et al. (2015) DAP12 stabilizes the C-terminal fragment of the triggering receptor expressed on myeloid cells-2 (TREM2) and protects against LPS-induced pro-inflammatory response. *J Biol Chem* 290:15866–15877.
12. Wang Y, et al. (2016) TREM2-mediated early microglial response limits diffusion and toxicity of amyloid plaques. *J Exp Med* 213:667–675.
13. Yuan P, et al. (2016) TREM2 haplodeficiency in mice and humans impairs the microglia barrier function leading to decreased amyloid compaction and severe axonal dystrophy. *Neuron* 92:252–264.
14. Ulland TK, et al. (2017) TREM2maintains microglial metabolic fitness in Alzheimer's disease. *Cell* 170:649–663.e13.
15. Zheng H, et al. (2017) TREM2 promotes microglial survival by activating Wnt/β-catenin pathway. *J Neurosci* 37:1772–1784.
16. Zhong L, et al. (2017) Soluble TREM2 induces inflammatory responses and enhances microglial survival. *J Exp Med* 214:597–607.
17. Cheng-Hathaway PJ, et al. (2018) The Trem2 R47H variant confers loss-of-function-like phenotypes in Alzheimer's disease. *Mol Neurodegener* 13:29.
18. Song WM, et al. (2018) Humanized TREM2 mice reveal microglia-intrinsic and -extrinsic effects of R47H polymorphism. *J Exp Med* 215:745–760.
19. Yuan P, et al. (2016) TREM2 haplodeficiency in mice and humans impairs the microglia barrier function leading to decreased amyloid compaction and severe axonal dystrophy. *Neuron* 90:724–739.
20. Roussos P, et al. (2015) The triggering receptor expressed on myeloid cells 2 (TREM2) is associated with enhanced inflammation, neuropathological lesions and increased risk for Alzheimer's dementia. *Alzheimers Dement* 11:1163–1170.
21. Piccio L, et al. (2016) Cerebrospinal fluid soluble TREM2 is higher in Alzheimer disease and associated with mutation status. *Acta Neuropathol* 131:925–933.
22. Leyns CEG, et al. (2017) TREM2 deficiency attenuates neuroinflammation and protects against neurodegeneration in a mouse model of tauopathy. *Proc Natl Acad Sci USA* 114:11524–11529.
23. Nimmerjahn A, Kirchhoff F, Helmchen F (2005) Resting microglial cells are highly dynamic surveillants of brain parenchyma in vivo. *Science* 308:1314–1318.
24. Davalos D, et al. (2005) ATP mediates rapid microglial response to local brain injury in vivo. *Nat Neurosci* 8:752–758.
25. Jung S, et al. (2000) Analysis of fractalkine receptor CX(3)CR1 function by targeted deletion and green fluorescent protein reporter gene insertion. *Mol Cell Biol* 20:4106–4114.
26. Guerreiro RJ, et al. (2013) Using exome sequencing to reveal mutations in TREM2 presenting as a frontotemporal dementia-like syndrome without bone involvement. *JAMA Neurol* 70:78–84.
27. Zhang Y, et al. (2014) An RNA-sequencing transcriptome and splicing database of glia, neurons, and vascular cells of the cerebral cortex. *J Neurosci* 34:11929–11947.
28. Rayaprolu S, et al. (2013) TREM2 in neurodegeneration: Evidence for association of the p.R47H variant with frontotemporal dementia and Parkinson's disease. *Mol Neurodegener* 8:19.
29. Yoshiyama Y, et al. (2007) Synapse loss and microglial activation precede tangles in a P301S tauopathy mouse model. *Neuron* 53:337–351.
30. Jicha GA, Bowser R, Kazam IG, Davies P (1997) Alz-50 and MC-1, a new monoclonal antibody raised to paired helical filaments, recognize conformational epitopes on recombinant tau. *J Neurosci Res* 48:128–132.
31. Paloneva J, et al. (2002) Mutations in two genes encoding different subunits of a receptor signaling complex result in an identical disease phenotype. *Am J Hum Genet* 71:656–662.
32. Haynes SE, et al. (2006) The P2Y12 receptor regulates microglial activation by extracellular nucleotides. *Nat Neurosci* 9:1512–1519.
33. Mazaheri F, et al. (2017) TREM2 deficiency impairs chemotaxis and microglial responses to neuronal injury. *EMBO Rep* 18:1186–1198.
34. Asai H, et al. (2015) Depletion of microglia and inhibition of exosome synthesis halt tau propagation. *Nat Neurosci* 18:1584–1593.
35. Krabbe G, et al. (2017) Microglial NFκB-TNFα hyperactivation induces obsessive-compulsive behavior in mouse models of progranulin-deficient frontotemporal dementia. *Proc Natl Acad Sci USA* 114:5029–5034.